Two-phase coexistence and semimetallic states in conducting polymers

M. I. Salkola
Theoretical Division, Los Alamos National Laboratory, Los Alamos, New Mexico 87545

S. A. Kivelson
Department of Physics, University of California, Los Angeles, California 90024
(Received 31 May 1994)

We study a simple model of conducting polymers, such as polyacetylene, which consists of a quasi-one-dimensional coupled electron-phonon system with short-range electron-electron repulsions. The problem is solved in the Hartree-Fock approximation. A variety of experimentally measurable properties of the system, especially the infrared absorption spectrum, are computed. (i) As a function of doping, the interchain coupling causes the system to undergo a phase transition from a correlated soliton-lattice state to a metallic state, described by a weakly interacting but highly anisotropic three-dimensional Fermi liquid. The result is consistent with a previous renormalization-group treatment. (ii) When interactions with counterions are included, the nonmetal–metal transition is very sensitive to the arrangement of counterions relative to the polymer chain: a minor change in the arrangement will either stabilize or destabilize the soliton state allowing the coexistence of the metallic and the soliton states. (iii) For realistic three-dimensional band structures, a semimetallic phase intervenes the nonmetallic (Peierls) and metallic (Fermi-liquid) phases.

I. INTRODUCTION

During the last decade, remarkable progress has been made in understanding the properties of conducting polymers.[1] Due to their quasi-one-dimensional nature, many of these materials in their pristine state have a Peierls or charge-density-wave ground state. Calculations based on a simple tight-binding Hamiltonian, proposed by Su, Schrieffer, and Heeger[2] (the SSH model), have been exceptionally successful in explaining the experimental results for several such polymers. For example, adopting their model for conducting polymers, one is naturally lead to a concept of novel quasiparticles, solitons, which have reversed charge-spin relations: the charged solitons have charge $\pm e$ but they have no spin and vice versa. The practical significance of these quasiparticles is that upon doping an added electron or hole appears as a charged soliton. Consequently, there exist states of the lightly doped polymer which can carry charge current (albeit poorly) without showing any spin susceptibility, as has been observed experimentally. Moreover, a distinctive infrared spectrum provides additional strong evidence for the validity of the theory; the solitons—as defects breaking the translational symmetry of the ground state—induce characteristic localized infrared-active phonon modes around them.

In spite of the successes of the theory, several important open questions still remain, of which the most pressing is the proper identification of the "metallic" state which appears in doped polymers when the doping density is increased above a critical value y_c (in polyacetylene, $y_c \sim 5-7\,\%$). This state is metallic in the sense that it has a high conductivity[3] (signifying charged quasiparticles with a long mean free path), a temperature-independent (Pauli) spin susceptibility[4] (quasiparticles have spin), and a linear specific heat. The magnitudes of the spin susceptibility and the specific heat are consistent with what would be expected from the density of states at the Fermi energy for a simple noninteracting metal. These *are* classic signatures of a normal Fermi liquid. Yet, in the metallic regime, the system continues to exhibit distinctive infrared-active modes which have been attributed to the presence of solitons and thus suggest that the state still has a nonzero Peierls gap.[5]

To resolve this apparent paradox, it has been proposed that disorder forces the system to undergo a crossover transition from an incommensurate charge-density-wave state to a gapless Peierls state.[6] The basic problem with this model is that it is difficult to reconcile the long observed mean free paths with the large amount of disorder needed to completely destroy the Peierls gap. On the other hand, Conwell and Jeyadev[7] argue that the metallic state can be reasonably well described by a model in which the added electrons or holes are in soliton states and the Coulomb potential of the counterions and the solitons in other chains cause a redistribution of the energy of the states in the Peierls gap. Their calculation is, however, not self-consistent since they assume a fixed soliton configuration. We feel it likely that a self-consistent solution will make the soliton lattice indistinguishable from a disordered, incommensurate Peierls state.

Furthermore, the applicability of the SSH model itself has been questioned.[8] The criticism relies on the argument that the electron-electron interaction determines the basic properties of the system and hence it is more important than the electron-phonon coupling. While this viewpoint certainly has merit if one is dealing with the true microscopic interactions, it is not clear what it means in terms of the low-energy, long-wavelength behavior of the system. Calculations which treat the in-

0163-1829/94/50(19)/13962(12)/$06.00

teractions from an *ab initio* viewpoint are necessarily confined to small systems (less than 20 sites) and so cannot possibly explore precisely those low-energy properties of the polymers of most interest to physicists. They also cannot easily include the effects of interchain screening.

We choose the point of view that typical conducting polymers, of which we consider *trans*-polyacetylene as an example, are in the scaling limit where the low-energy physics is described by a Hamiltonian with a few relevant interactions; the parameters entering into the model are thus *renormalized* ones. Indeed, the renormalization-group theory shows that the system scales towards a strong-coupling fixed point where the electron-phonon coupling is the dominant coupling *regardless* of the relative strength of the microscopic interactions.[9] (Since we will be dealing with renormalized parameters it is important to bear in mind that the effective interactions can be complicated functions of the bare interactions, and can even depend on doping density.) Strictly speaking the scaling equations are valid only close to the noninteracting fixed point, so while this approach permits us to treat arbitrary relative strengths of the different interactions, we are forced to assume that all interactions are moderately weak. The interactions in polyacetylene and related polymers are at least moderately weak, as evidenced by the small gap-to-bandwidth ratio in the undoped material, so the scaling theory should be at least qualitatively correct.

In this spirit, it seems reasonable to study a quasi-one-dimensional coupled electron-phonon system, supplemented by short-range electron-electron repulsion, as a model for *trans*-polyacetylene. It is the purpose of this paper to demonstrate that at the mean-field level the model exhibits a phase transition from the Peierls state to a metallic state which is characterized by a weakly interacting but highly anisotropic Fermi liquid. The transition happens when the gap becomes comparable to the interchain bandwidth in which case the true three-dimensional nature of the system becomes the dominant feature in the problem. Moreover, the inclusion of impurities (i.e., counterions) strongly affects the critical value of the doping density. A minor change in the arrangement of impurities relative to the polymer chain will either stabilize or destabilize the soliton state allowing the coexistence of the metallic state and the soliton state within the same sample. This result provides a possible explanation of why in the metallic regime the system can have both the high Pauli susceptibility and still exhibit the infrared-active modes characteristic of the soliton state.

There is another process which can account for a part of the total oscillator strength of the infrared-active modes in metals: the Holstein process in which the incident photon is absorbed in a process involving creation of both a phonon and an electron-hole pair.[10] This is a purely nonadiabatic effect. In contrast, the infrared properties of the incommensurate Peierls state are typically calculated within the adiabatic approximation, which is only valid when the optical-phonon energy is much smaller than the energy gap in the electronic spectrum.

The outline of this paper is as follows. In Sec. II, we introduce the effective Hamiltonian, discuss the strategy for solving it in the mean-field approximation, and exhibit our method for correcting for finite-size effects. Next, the best Hartree-Fock ground state is computed in the presence of counterions (Sec. III). We find that, in a highly doped system, counterions have a drastic influence on the ground-state properties. In Sec. IV, the absorption in the Peierls state is calculated in the adiabatic limit. At low doping, the charge is pinned, which leads to a suppression of the infrared oscillator strength. Thus, there can be regions of *superlinear* dependence of the infrared oscillator strength on doping density. The pinning is lost when the doping density is increased above 3–6 %, depending on the preparation of the sample. We also study nonadiabatic corrections (Holstein processes) which can produce strong absorption peaks in metals due to the dynamic electron-phonon interaction. Section V is devoted to three-dimensional effects, especially to the effect of a finite three-dimensional bandwidth. Finally, in Sec. VI, we discuss our results in the context of polyacetylene and the Appendixes contain the details of the calculations.

II. GENERAL FORMALISM

A. Effective Hamiltonian

Given a microscopic Hamiltonian—a faithful description of *trans*-polyacetylene—how can we determine the ground-state properties of the system, at least within a reasonable approximation? It is hardly possible to solve the full microscopic problem in a controlled fashion, but a simple effective model can be constructed, whose properties are easily understood if only low-energy phenomena are to be studied.[11] The renormalization-group theory demonstrates[9] that there exists an effective Hamiltonian with a few renormalized interactions (of which the electron-phonon coupling is the dominant one), if certain conditions are fulfilled: notably, if the electron-phonon interaction is sufficiently retarded (the phonon energies are small compared to all other energies) and if the ratio of the largest energy gap to the bandwidth is small enough. In undoped polymers, where the ratio of the gap to the bandwidth is about $\frac{1}{5}$, these conditions are marginally well satisfied; in highly doped polymers, where the gap collapses, these conditions are extremely well satisfied.

In this framework, consider a one-dimensional electron gas interacting with a deformable chain, described by the Hamiltonian

$$H=-\sum_{n\sigma}[t_0+\alpha(u_n-u_{n+1})](c^{\dagger}_{n+1\sigma}c_{n\sigma}+\text{H.c.})+\frac{1}{2}\sum_{nn'}V_{n-n'}\rho_n\rho_{n'}+V_I+\frac{1}{2}K\sum_n(u_n-u_{n+1})^2+\frac{1}{2M}\sum_n p_n^2\,, \tag{2.1}$$

where $c^{\dagger}_{n\sigma}$ and $c_{n\sigma}$ are the creation and annihilation

operators of an electron of spin σ on site n, $\rho_n = \sum_\sigma c_{n\sigma}^\dagger c_{n\sigma}$ is the electron number density operator on site n, and u_n is the displacement of the nth CH group. Here t_0 is the electron hopping matrix element for the undistorted chain, α is the electron-phonon coupling constant, K is the spring constant, M is the mass of the CH group, V_n is the electron-electron interaction, and V_I is the potential due to the counterions. If $V_n = U\delta_{n,0}$ and $V_I = 0$, this is the SSH-Hubbard model. The electron-phonon interaction is characterized by the dimensionless coupling constant

$$\lambda = \frac{2\alpha^2}{\pi K t_0} . \tag{2.2}$$

The renormalized parameters appearing in the Hamiltonian can be expressed as complicated functions of the bare parameters.[9] However, it is simpler to determine them empirically by comparing the effective theory with experiments. Finally, the number of electrons is given by the doping density y, which measures the number of added holes (p-type) or electrons (n-type) relative to the half-filled (one electron per site) system. In the subsequent calculations, p-type doping is always assumed for simplicity.

In the absence of the electron-electron interactions and the counterion potential, the properties of the Hamiltonian (2.1) are well known.[1] Upon doping, the system generates a periodic incommensurate Peierls distortion. At low doping levels, the distortion is highly anharmonic and can be best thought of as an array of well-defined solitons. When the doping density, y, is high enough, the solitons lose their identity and a new collective state, better described as a harmonic incommensurate charge-density wave, emerges. The crossover occurs when the separation between the solitons becomes comparable to their width, 2ξ. The characteristic doping density at which this crossover occurs is $y_* = a/2\xi$. For polyacetylene, the SSH set of parameters[12] give $y_* \simeq 7\%$.

Clearly three-dimensional effects have been ignored in Hamiltonian (2.1). They are, however, important when the transverse bandwidth becomes comparable to the energy gap. At this point, the behavior of the system crosses over from one dimensional to three dimensional. While we assume no interchain coupling for the moment, we will return to this question later in Sec. V.

B. Mean-field approximation

Even the effective Hamiltonian given above cannot be solved exactly, and therefore approximate methods must be used. A standard technique to tackle the problem is mean-field theory, i.e., the Hartree-Fock approximation. It relies on two key assumptions: (i) the ionic coordinates can be treated classically and (ii) the ground state can be approximated by a product of one-electron states. In this manner, the problem becomes completely solvable.

However, by doing this we have ignored all effects of quantum and thermal fluctuations which are known to be important in one dimension. Thermal fluctuations will typically be unimportant for the systems we are considering, since all relevant experimental temperatures are very low compared to the characteristic scale of energy. Quantum fluctuations are a more serious issue, but we feel that their neglect can, ultimately, be justified in certain circumstances by a comparison between the mean-field and renormalization-group results.

The Hartree-Fock variational state can most simply be constructed[13] by finding the ground state of the trial Hamiltonian

$$H_0 = -\sum_{n\sigma} [t_0 + \alpha(u_n - u_{n+1})](c_{n+1\sigma}^\dagger c_{n\sigma} + \text{H.c.}) + V_I + \sum_n x_n \rho_n + \frac{1}{2} K \sum_n (u_n - u_{n+1})^2 , \tag{2.3}$$

where x_n and the chain distortion, u_n, are treated as variational parameters which specify the ground state $|\psi\rangle$. Here we consider only solutions of the Hartree-Fock equations which preserve spin-rotational symmetry, because, in one dimension, quantum fluctuations are so large that the ground state must have unbroken spin-rotational symmetry.[14] Other than this, no assumptions are made concerning the symmetry of the ground state. The best variational ground state is obtained by minimizing the total energy

$$\begin{aligned} E &= \langle\psi|H|\psi\rangle \\ &= \langle\psi|H_0|\psi\rangle - \sum_n x_n \langle\psi|\rho_n|\psi\rangle \\ &\quad + \frac{1}{2}\sum_{nn'} V_{n-n'} \langle\psi|\rho_n\rho_{n'}|\psi\rangle , \end{aligned} \tag{2.4}$$

with respect to x_n and u_n.

C. Remarks on finite-size scaling

While an analytic solution to the minimum-energy condition can be found in a limited number of cases, generally the minimization must be carried out numerically. However, numerical calculations are restricted to finite systems. Therefore one cannot immediately distinguish a gapless state from a state whose energy gap is of same order of magnitude or less than the level spacing, $\delta\epsilon_N$, at the Fermi energy where, in ring geometry,

$$\delta\epsilon_N = \frac{4\pi}{N} t_0 \cos k_F a ; \tag{2.5}$$

N is the number of lattice sites, k_F is the wave vector at the Fermi energy, and a is the lattice constant. For instance, if we were to study polyacetylene in conditions where the physical gap is known to be 0.2 eV, then the length of the ring must be longer than 160 sites to guarantee that finite-size effects do not affect the conclusions. Because we are primarily interested in cases where the energy gap (the minimum energy to create an electron-hole pair) is very small or zero, we must employ finite-size scaling arguments to obtain results that are valid in the thermodynamic limit.

There is a qualitative difference between rings containing an even number of sites depending whether N is $4n$ or $4n+2$.[13] This difference arises from the band structure

of the undistorted finite-size ring (H_0 with $u_n = x_n = 0$) in which other than the states at the top and the bottom of the band, all one-electron states are two-fold degenerate (Kramers degeneracy). For fixed density of electrons on a ring, the Fermi energy will either lie in a finite-size gap (the "nondegenerate case") or will be equal to the energy of a partially occupied one-electron state (the "degenerate case"). In the degenerate case it is always energetically favorable for the system to generate a Jahn-Teller distortion which lifts the degeneracy and produces a gap. By contrast, in the nondegenerate case, there exists a critical length of the ring such that if the length is less than the critical value it will remain undistorted. The smaller the Peierls gap in the thermodynamic limit, the larger the critical length. If the Peierls gap is very small then—due to the computational limitations on N—we cannot get enough data to observe the Peierls effect in nondegenerate rings. In contrast, the finite-size behavior in the degenerate case is not hampered by the same deficiency. Of course, in the limit $N \to \infty$, it cannot matter how the limit is approached. For degenerate finite-size rings, we find that so long as the gap, $2\Delta_N$, is smaller than the level spacing, $\delta\epsilon_N$, the energy gap decreases linearly with decreasing $1/N$:

$$\Delta_N = \tilde{\Delta}_\infty + \frac{c}{N} + \mathcal{O}\left[\frac{1}{N^2}\right], \tag{2.6}$$

where $\tilde{\Delta}_\infty$ and c are constants. When the energy gap becomes comparable to the level spacing, it levels off and approaches its $N \to \infty$ limit $2\Delta_\infty$ which is approximately equal to $2\tilde{\Delta}_\infty$.

III. COUNTERION EFFECTS

The doping process itself introduces charged impurities, counterions (usually one per added hole or electron). At low doping density, one can study how a single counterion changes the properties of conducting polymers. However, at higher doping densities, the counterions must be considered collectively, and the system shows striking behavior which is due to the topological nature of the Peierls state. Moreover, above the crossover density y_*, the energy gap begins to collapse and the Peierls state is no longer robust against small perturbations.

A. Counterion potential

The counterions are described by the term

$$V_I = \sum_n v(n)\rho_n , \tag{3.1}$$

where v can be expressed as a sum of a long-range part, v_C, which is given by a dielectrically screened Coulomb interaction, and a short-range term, v_0, due to the incomplete screening at short distances. Thus,

$$v(n) = v_C(n) + v_0(n) , \tag{3.2}$$

where v_C is

$$v_C(n) = \frac{e^2}{\epsilon_\perp} \sum_{\mathbf{R}} \frac{1}{\sqrt{(na - R_\parallel)^2 + (\gamma R_\perp)^2}} . \tag{3.3}$$

Here $\mathbf{R}$ labels the position of the counterions, $\perp$ ($\parallel$) refers to the direction perpendicular (parallel) to the chain axis, and $\gamma = \sqrt{\epsilon_\parallel/\epsilon_\perp}$. $\epsilon_\parallel$ and $\epsilon_\perp$ are the anisotropic dielectric constants of the material.[15] The term v_0 is a sum over all counterions interacting with the electrons at the nearest one or two carbon atoms of each counterion.

The three-dimensional crystal structure of counterions in moderately doped polyacetylene is such that the impurity ions are displaced from the chains by a distance $b \simeq 2.3$ Å in the direction perpendicular to the chain axis and there is one column of counterions for several polyacetylene chains; for instance, in Na-doped polyacetylene there are three polymers per counterion chain.[16] Thus, we will consider a periodic arrangement of counterions with lattice constant l in the inchain direction, $l = a/(3y)$. It is important to note that this period is smaller than the lattice constant of the expected soliton lattice, a/y.

While the screened Coulomb potential can be fairly strong in the lightly doped system, it is entirely negligible at metallic densities: only the short-range unscreened part of v plays any role in the physics. We show this by using the Poisson summation formula to rewrite Eq. (3.3) as

$$v_C(n) = \frac{4e^2}{\epsilon_\perp l} \sum_{q=1}^{\infty} \cos(2\pi nqa/l) \sum_{\mathbf{r}} K_0(2\pi\gamma q|\mathbf{r}|/l) + \text{const} , \tag{3.4}$$

where n labels a particular carbon atom along a given chain and the sum over $\mathbf{r}$ is over the perpendicular displacement of the columns of counterions. K_0 is the modified Bessel function of the second kind. Its most important property needed here is that $K_0(z) \simeq e^{-z}\sqrt{\pi/2z}$, for $z \gg 1$. Hence,

$$v_C(n) \simeq \frac{2e^2}{\epsilon_\perp l} \cos(2\pi na/l)\sqrt{l/\gamma b}\, e^{-2\pi\gamma b/l} + \text{const}, \tag{3.5}$$

when $2\pi\gamma b/l \gg 1$. Already in 6%-doped polyacetylene, $2\pi\gamma b/l = 3.8$, so v_C is negligibly small. (This argument is similar to the argument of Kivelson and Heeger[17] for the insensitivity of the transport properties to disorder in the arrangement of the counterions.) The peak-to-trough value v_p, defined as $v_p = \max_x v_C(x) - \min_x v_C(x)$ and shown in Fig. 1, drops sharply at the doping density given as $\sim a/(6\pi\gamma b)$. For polyacetylene, this doping density is approximately 1.6%.

The lesson of all this is that, while the energy gap collapses at the crossover density, y_*, the dielectrically screened Coulomb potential drops much faster and is always negligible at metallic densities. Therefore, one is left only with the short-range Coulomb interactions. In the following, we assume that these have the simple form

$$v_0(n) = v_I \sum_R \delta_{R,n} , \tag{3.6}$$

where v_I is the strength of the potential and R runs over

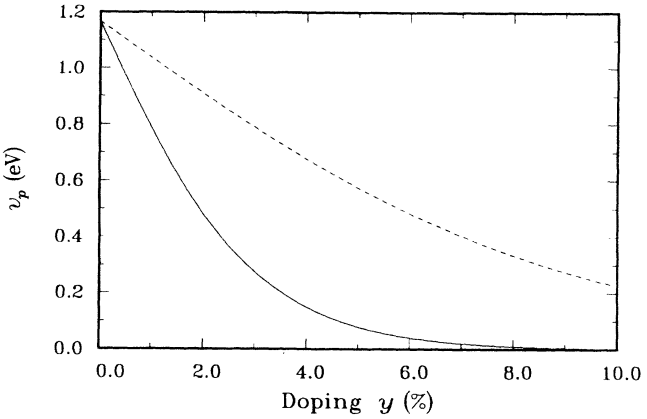

FIG. 1. The peak-to-trough value v_p of the dielectrically screened impurity potential, Eq. (3.3), on a polyacetylene chain as a function of doping, y, when the separation between counterions is $l=a/(3y)$ (——) and $l=a/y$ (— — —).

the lattice sites closest to the counterions and we take the counterions to be, more or less, regularly arranged with a mean separation $l=a/(3y)$.

B. Numerical results

An ordered array of counterions does not change the basic nature of the mean-field phase diagram, but the short-range counterion potential can have a large effect on the location of the phase boundaries. Depending on the local arrangement of the counterions relative to the polymer chain, we find that the critical doping density for the nonmetal–metal transition, y_c, can be either substantially enhanced or substantially reduced from its value in the absence of the counterion potential.

One can qualitatively understand this effect simply by thinking about the electronic structure of a soliton lattice: the soliton is a topological defect, and this is responsible for a number of its remarkable properties. In the context of the SSH model, it is found that the charge density is zero on odd numbered sites and nonzero only on even numbered sites, regardless of the position of the soliton center, and conversely for the antisoliton:[18] there are two length scales, ξ and a, associated with the size and the internal structure of the soliton. Although electron-electron interactions modify this result, it remains true that the soliton charge density is predominantly on even sites and the antisoliton is predominantly on odd sites.[13] In the soliton lattice, it is topologically necessary that the solitons and antisolitons alternate. If the short-range part of the counterion potential, v_0, is such that in the neighborhood of the solitons it is attractive on odd numbered sites, then the soliton lattice is greatly stabilized. On the other hand, if the opposite is true, the soliton lattice is destabilized. In the former case, the topological constraint allows the solitons and antisolitons to adjust their position relative to the counterions so that there is a large electron density in regions where the potential energy due to the counterions is most attractive. This is not possible in the latter case where only the solitons or the antisolitons can locate in regions of low potential energy.

As the Peierls state starts to lose its robustness at y_*, phasing between the soliton and the impurity chains becomes a significant new element in the theory. To illustrate these ideas, we have done numerical calculations in some typical cases which should be applicable to *trans*-polyacetylene. These results are summarized in Figs. 2 and 3, based on the variational calculation of Sec. II for a fixed periodic array of counterions with period l.

The method of finite-size scaling study of Fig. 2 is shown for representative values of the parameters: doping density $y=6.67\%$, $U=t_0$, and $v_I=t_0$. In these calculations, N is $30n$ and the number of holes is $2n$, where $n=1,\ldots,5$. We study the effect of the counterion spacing l by considering the cases $l=4a$, $l=5a$ [$l=a/(3y)$], and $l=6a$. All continuous curves in Fig. 2 are straight lines[19] which reflect the linear scaling behavior, Eq. (2.6), for small N so long as $2\Delta_N<\delta\epsilon_N$.

In all cases, the gap $2\Delta_N$ decreases linearly with decreasing $1/N$ until it becomes comparable to the level spacing, $\delta\epsilon_N$, at which point it saturates. This value is interpreted as a true gap of the infinite system. For the sake of comparison, we compute the scaling trajectory in the nondegenerate case with $l=5a$. Here, for small N, the trajectory follows the level spacing $\delta\epsilon_N$ until it becomes comparable to the gap of the infinite system at which point it also saturates. Moreover, the difference between the degenerate and nondegenerate case disappears as $N\to\infty$.

It is clear that the arrangement of the counterions also affects the energy gap: if the counterions are located alternately next to the odd and even sites, the gap is enhanced; if the counterions are always located next to

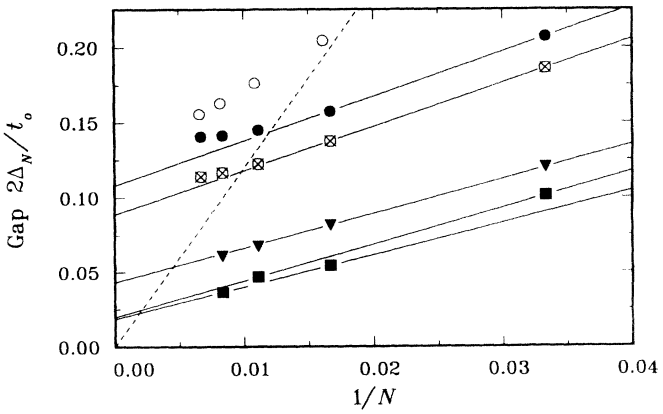

FIG. 2. Determination of the energy gap, $2\Delta_\infty$, by finite-size scaling. The parameters are $y=6.67\%$, $U=t_0$, and $v_I=t_0$. The influence of the counterions on the energy gap is illustrated by using three different values for the separation l between the counterions: $l=4a$ (■), $l=5a$ (●), and $l=6a$ (▼). Also, for $l=5a$, a comparison between the degenerate (●) and the nondegenerate (○) cases is shown. (All solid symbols refer to the degenerate cases.) The counterion-free case is marked by (⊗). The finite-size level spacing $\delta\epsilon_N$, defined in Eq. (2.5), is denoted by the dashed line.

the even (or odd) sites, the gap is suppressed. This follows from the topological constraint to the positions of solitons and antisolitons, as already explained above. Thus, even if the average impurity density is homogeneous in a given sample, the metallic and Peierls states can coexist due to subtle microscopic differences in the arrangement of the counterions in different regions of the material and due to the interchain coupling. As it will be shown in Sec. V, the metallic state is stabilized, if the one-dimensional energy gap is less than a critical value, determined by the three-dimensional band structure of the system.

We have also calculated the energy gap, 2Δ, and the average amplitude of the bond-length modulation, $\delta\bar{u}$, as a function of doping density, y (Fig. 3). The average amplitude is defined as

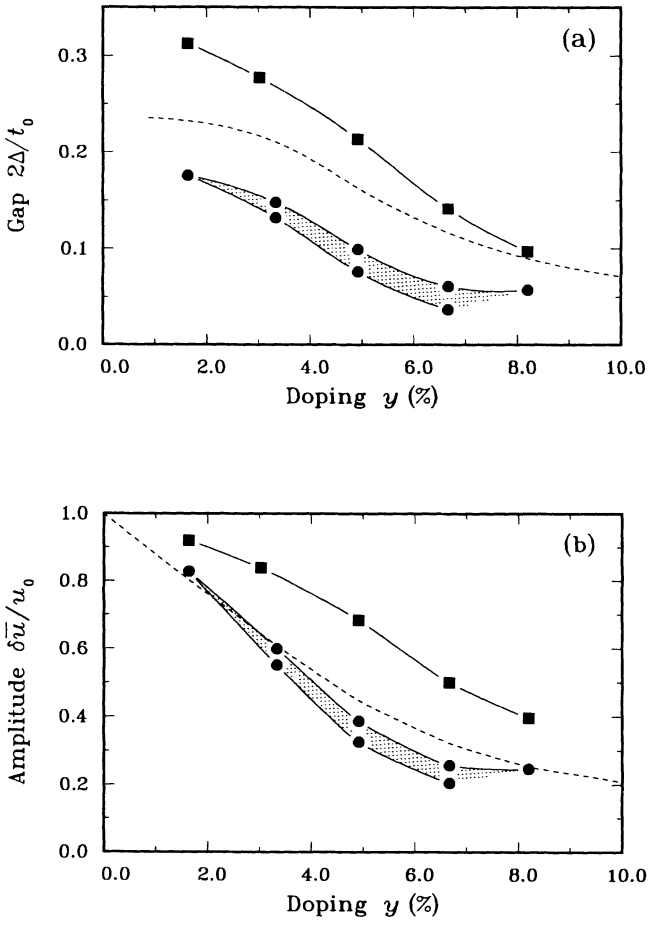

FIG. 3. (a) The energy gap 2Δ and (b) the average amplitude of the Peierls distortion, $\delta\bar{u}$, as a function of doping density, y, for $U=t_0$ and $v_I=t_0$. The symbols are as follows: the dashed line denotes the counterion-free case, l/a=odd (■), and l/a=even (●), where l is the separation between counterions. Computations are based on those values of l which are summarized in Table I and approximately satisfy the relation $l=a/(3y)$. The shadowed regions emphasize the effect of changing l only by $2a$. Here $u_0=0.082$ Å is the magnitude of the lattice distortion for the half-filled band.

$$\delta\bar{u}=\frac{1}{N}\sum_n |u_{n+1}-u_n| \ . \tag{3.7}$$

For each y, the counterion lattice constant, l, has been chosen so that the relation $l=a/(3y)$ is approximately satisfied; see Table I. The cases l/a=odd and l/a=even are separated since their behavior is intrinsically different. For a weak counterion potential and y not too large, the results do not deviate much from the counterion-free case, but when the counterion potential is strong, a considerable deviation is found. Even a small change in l can produce a large effect which is illustrated by using two slightly different sets of even values for l/a, listed in Table I and indicated by the shadowed region in Fig. 3. In this figure, the upper boundary is the result for a counterion separation which is $2a$ units larger than the separation used in calculating the lower boundary (see Table I).

In these calculations, the size of the system, N, is either 120 or 122. Since for the systems of this size, the level spacing is smaller than the interchain bandwidth, we have not performed finite-size scaling (see Sec. V).

IV. INFRARED ABSORPTION

One of the greatest successes of the soliton concept is that it beautifully explains the enormous increase in the infrared activity induced by doping. Indeed, the infrared activity is considered to be an indisputable signature of a localized phonon mode which couples to the nonuniform charge density around a soliton. Our primary interest is to study whether counterions can cause an observable change in this infrared activity, and what becomes of it at higher doping levels.

A. Adiabatic limit

Suppose that the electronic spectrum has an energy gap of magnitude much larger than any phonon energy in the system. In this limit, one is naturally led to the Born-Oppenheimer approximation in which the electronic ground state, $|\psi\rangle$, is determined by the instantaneous lattice configuration and the electronic energy acts as an effective potential for the lattice dynamics. By expanding the interaction between the system and the electromagnetic field in powers of the phonon field, the infrared absorption is easily computed; see Appendix A. Our analysis is restricted strictly to one-dimensional lattices

TABLE I. The doping densities y and the corresponding counterion lattice constants l, as used in the numerical calculations and chosen so that the relation $l=a/(3y)$ is approximately obeyed.

y (%)	l/a odd	l/a even	
1.6	21	20	22
3.3	11	10	12
4.9	7	6	8
6.7	5	4	6
8.2	5	4	6
10.0	3	2	4

whereas a real polymer has additional vibrational degrees of freedom. For instance, *trans*-polyacetylene has three degrees of freedom which couple strongly to the charge distribution.[20] However, to understand the qualitative physics, it should be sufficient to study systems with one vibrational mode.

The numerical results are summarized in Fig. 4. Again, the parameters are chosen to represent polyacetylene[12] and the values for the separation between the counterions, l, are taken from Table I. In the absence of counterions, the integrated absorption increases linearly with the doping density for small y, while above $y \sim 6\%$ there is a small deviation from the linear behavior which is caused by the decrease of the energy gap, 2Δ. The linear part is most naturally given by the formula

$$\mathcal{A}_{\rm ad} = \frac{\pi}{2}\frac{Ny}{V}\frac{e^{*2}}{m^* c} , \tag{4.1}$$

which describes quasiparticles with effective charge e^*, effective mass m^*, and density Ny/V; c is the velocity of light. Here the quasiparticles clearly are solitons. Since the charge of a soliton is $e^* = e$, Eq. (4.1) gives an estimate for the effective mass: $m^* \simeq 3.7 m_e$, which is comparable to the kinematic mass of the soliton.[21]

This result arises naturally once Eq. (4.1) is interpreted as a low-energy sum rule which includes those processes whose energy scale is determined by the typical phonon energy, $\hbar\omega_0$. The existence of two distinct energy scales ($\hbar\omega_0$ and 2Δ) makes the above separation possible. When this separation ceases to exist (for $y > y^*$), the quasiparticle concept and the adiabatic approximation both break down.

Next, we add the interaction with the counterions, Eq. (3.6), so that the mean separation between the counterions, l, is approximately $a/(3y)$. For small values of y, the solitons are pinned to the counterions and $\mathcal{A}_{\rm ad}$ is suppressed. When l/a is an odd integer, the pinning is optimal since then it is topologically possible for each solitons to have its maximum charge density next to a counterion. Moreover, the pinning force increases with the increasing counterion potential v_I. Above $y \sim 6\%$, the pinning weakens and $\mathcal{A}_{\rm ad}$ increases considerably. However, the quasiparticle parameters are spurious since the effective charge e^* has changed too; only the ratio e^{*2}/m^* can be determined precisely with the given information.

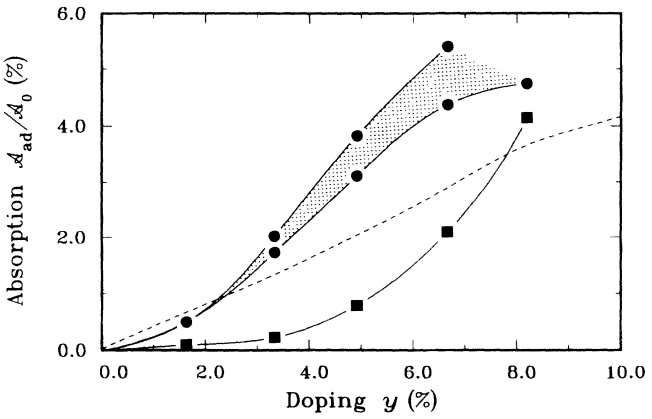

FIG. 4. The integrated absorption $\mathcal{A}_{\rm ad}$ for adiabatic processes as a function of doping density, y, for $U = t_0$, and $v_I = t_0$. The symbols are as follows: the dashed line denotes the counterion-free case, l/a=odd (■) and l/a=even (●). Computations are based on those values of the separation between counterions, l, which are summarized in Table I and approximately satisfy the relation $l = a/(3y)$. The shadowed regions emphasize the effect of a change of $2a$ in l. $\mathcal{A}_0$ is the total oscillator strength, Eq. (A10).

For l/a equal to an even integer, the pinning seems to disappear already at $y \sim 3\%$. Moreover, the impurity potential distorts the Peierls state strongly so that a large increase in $\mathcal{A}_{\rm ad}$ is observed. Again, for a large counterion potential, $v_I = t_0$, a sizable change in the absorption is found (the shadowed region in Fig. 4) even if l is altered by a small amount (shown in Table I). In contrast, for $v_I = t_0/2$ (not shown), a large effect is evident only when $y > 8\%$, which is due to the collapse of the energy gap and a large relative change in l. Above $y \sim 8\%$, these states are not well-defined Peierls states, and it is not guaranteed that they will survive the limit $N \to \infty$. In fact, they should be strongly modified by interchain coupling.

B. Nonadiabatic limit

Although conventional wisdom in polymer science always associates infrared-active modes with localized defects, such as solitons, normal metals, especially those with low conductivity, also show substantial infrared activity. Their ability to absorb radiation is partially due to the scattering from phonons and impurities. These phonon-assisted absorption processes, studied by Holstein,[10] have been seen in a number of materials.

We shall see below that, for simple one-dimensional metals, the absorption coefficient is proportional to the electron-phonon coupling constant λ whereas in insulators, the Holstein contribution is shifted in energy by 2Δ, and it is suppressed by an extra factor of $\hbar\omega_0/2\Delta$. Here $\hbar\omega_0$ is a typical optical-phonon energy and 2Δ is the energy gap. For undoped polyacetylene, this factor is of the order of $\frac{1}{10}$. However, near the insulator-metal transition, where the energy gap collapses, the Holstein process is effectively turned on and can partially account for the observed infrared oscillator strength. To illustrate this phenomenon, we compute the absorption coefficient for both a one-dimensional metal and an insulator.

1. *One-dimensional metal*

We assume that the system is described by the standard model of an electron gas interacting with the phonons, i.e., the Hamiltonian in Eq. (2.1) with $V_n \equiv 0$ and $V_I = 0$. In the lowest order of λ, it can be shown (see Appendix B) that the absorption coefficient is

$$\alpha_H(\omega) = \lambda \mathcal{A}_0 \frac{2\omega_0}{\omega^3}(\omega - \omega_0)\theta(\omega - \omega_0) . \tag{4.2}$$

In this limit, the integrated absorption due to the Hol-

stein process is equal to $\mathcal{A}_H=\lambda\mathcal{A}_0$, which is similar, e.g., to Allen's calculation.[22] The absorption coefficient, Eq. (4.2), is characterized by a peak which is located at the frequency $\omega_p=3\omega_0/2$.

As an illustration, consider polyacetylene which has $\lambda=0.2$. The integrated absorption due to nonadiabatic processes in the metallic state can be much higher than the absorption due to adiabatic processes in the Peierls state, despite the small value of λ. Two factors are responsible for this difference, as can be seen from the formula $\mathcal{A}_{\rm ad}\simeq y(m/m^*)\mathcal{A}_0$: (i) the soliton density ($y<y_*$) is necessarily much smaller than the full electron density (~ 1) and (ii) the soliton mass is larger than the electron band mass.

2. *One-dimensional insulator*

Due to the Peierls distortion, undoped polyacetylene has an energy gap of a few eV. The energy gap is large enough that the adiabatic approximation is applicable for calculating infrared properties of the system. Also, it is large enough to suppress the Holstein processes effectively.

Given that the chain has a dimerized ground state with an energy gap of 2Δ, one can diagonalize that part of the Hamiltonian which contains the kinetic energy of the electrons plus the interactions between the electrons and the macroscopically occupied phonon modes with $q=\pm\pi/a$. The rest of the Hamiltonian is then treated as a small perturbation; i.e., the residual part of the electron-phonon interactions. Due to the unitary transformation which diagonalizes the mean-field Hamiltonian, the electron-phonon and also the electron-photon interactions are changed. Again, no electron-electron nor counterion interactions are considered.

Without going into details, we quote the result which is

$$\alpha_H(\omega)=2\lambda\frac{\omega_0}{\Delta^2}\mathcal{A}_0 I(\omega)\theta(\omega-\omega_0-2\Delta) \tag{4.3}$$

to first order of λ. The profile factor I is defined as

$$I(\omega)=\frac{1}{(\varphi+\eta)^3}\times\int_1^{\varphi/2}dx\left[\frac{\sqrt{x^2-1}}{2x}\frac{\varphi-x}{\sqrt{(\varphi-x)^2-1}}+\frac{x}{2\sqrt{x^2-1}}\frac{\sqrt{(\varphi-x)^2-1}}{\varphi-x}+1\right], \tag{4.4}$$

where $\varphi=(\omega-\omega_0)/\Delta$ and $\eta=\omega_0/\Delta$. In the limit $\omega_0\ll\Delta$, the integrated absorption can be expressed in a simple form:

$$\mathcal{A}_H\simeq\left[\frac{\omega_0}{2\Delta}\right]\lambda\mathcal{A}_0 . \tag{4.5}$$

As promised, $\mathcal{A}_H$ is suppressed by a factor of $\omega_0/2\Delta$ from its zero-gap value. For polyacetylene, this factor is about $\frac{1}{10}$. It is important to realize that this contribution to the absorption is mingled with the electronic transitions: it does not appear in the energy gap.

V. THREE-DIMENSIONAL EFFECTS

There is growing evidence—both experimental[4,23] and theoretical[9,17]—that the interchain coupling is ultimately responsible for genuine metallic behavior of the highly doped polymers. The renormalization-group theory shows that the Peierls instability generates an energy gap in a one-dimensional system so long as the largest phonon energy, $\hbar\omega_0$, is small compared to the single-particle gap energy, 2Δ, and the intrachain bandwidth, $W_\parallel=4t_0$, is much larger than 2Δ. Even the mean-field theory which ignores strong-fluctuation effects in one dimension is in qualitative agreement. But when 2Δ becomes comparable to the interchain bandwidth, $W_\perp$, the system crosses over to a truly three-dimensional system. Moreover, depending on microscopic details, the Peierls instability is either partially or completely inhibited when 2Δ is comparable to or smaller than $W_\perp$.

In the following, we assume that the Coulomb interaction between electrons has already been accounted for in the renormalized values of the relevant physical parameters and that the remaining residual interactions are small enough to be ignored. Also, from now on, we neglect the counterion effects and consider only cases where $\hbar\omega_0<W_\perp\ll W_\parallel$.

A. Ferromagnetic ordering of the Peierls state

To begin with, we assume ferromagnetic ordering of the Peierls state on adjacent chains, i.e., we assume that the charge-density waves on adjacent chains are in phase with each other. It is straightforward to demonstrate (see Appendix C) that, as a function of Δ and for a given $W_\perp$, the total energy $E_T(\Delta;W_\perp)$ per electron has at least two local minima at (i) $\Delta\neq 0$, $W_\perp=0$ and (ii) $\Delta=0$, $W_\perp\neq 0$. At these points, the total energy is

$$E_T(\Delta_0;0)=E_T(0;0)-\frac{\Delta_0^2}{\pi W_\parallel} , \tag{5.1}$$

and

$$E_T(0;W_\perp)=E_T(0;0)-\zeta\frac{W_\perp^2}{\pi W_\parallel} . \tag{5.2}$$

Here $2\Delta_0$ denotes the order parameter, equal to the energy gap, of the one-dimensional system, whereas 2Δ is the order parameter of the corresponding three-dimensional system; both Δ_0 and Δ depend on doping density y. The factor ζ is the second moment of $\rho_\perp$ in dimensionless form

$$\zeta=\frac{2}{W_\perp^2}\int_{-\infty}^{\infty}d\epsilon\,\epsilon^2\rho_\perp(\epsilon) . \tag{5.3}$$

Note that ζ must lie in the range

$$0\le\zeta\le\tfrac{1}{2} . \tag{5.4}$$

The interesting result is that, depending on the value of ζ, there is either a first- or second-order transition to a

metallic state. To relate this to experiment, we use our previous renormalization-group results for a one-chain model according to which the effective electron-phonon coupling constant, and hence the one-dimensional single-particle energy gap $2\Delta_0$, are decreasing functions of the doping density y. (i) If $\zeta > \frac{1}{4}$ and $2\Delta_0 < W_\perp\sqrt{4\zeta}$, the metallic state has lower energy than the Peierls state. Thus, the system undergoes a first-order transition from the nonmetallic Peierls state to the metallic state at $2\Delta_0 = W_\perp\sqrt{4\zeta}$. (ii) if $\zeta < \frac{1}{4}$, the order parameter 2Δ decreases continuously to zero and the transition is second order. In this region and for $2\Delta_0 < W_\perp$, the system has a finite density of states at the Fermi energy, but the Fermi surface is incomplete. As Δ_0 decreases below a critical value Δ_0^c, determined by $W_\perp$, the Peierls state is completely suppressed and the system becomes fully metallic, $\Delta = 0$. [Remember that Δ_0 signifies the value of Δ in the limit $W_\perp \to 0$ and that $\Delta_0 = \Delta_0(y)$.] A naive comparison of Eqs. (5.1) and (5.2) shows that $\Delta_0^c \leq W_\perp\sqrt{\zeta}$. Conversely, for a given Δ_0, there exists a critical value $W_\perp^c$ such that, for $W_\perp \geq W_\perp^c$, the metallic state is stabilized.

As an example in which the transition is continuous, let $\rho_\perp(\epsilon)$ be a constant, implying $\zeta = \frac{1}{6}$. Now, suppose that the doping density is high enough so that the midgap band is fully developed. Then it is adequate to take

$$\rho_\parallel(\epsilon) = \frac{2}{W_\parallel}\frac{|\epsilon|}{\sqrt{\epsilon^2-\Delta^2}}\theta(\epsilon^2-\Delta^2)\ . \tag{5.5}$$

Let $2\Delta_0 \leq W_\perp$ and expand the total energy in a Taylor series at the point $\Delta = 0$. The total energy has a minimum at $\Delta \neq 0$, for $\Delta_0 > \Delta_0^c$, where

$$2\Delta_0^c \equiv \left[\frac{2}{e}\right] W_\perp\ , \tag{5.6}$$

and at $\Delta = 0$, for $\Delta_0 \leq \Delta_0^c$. Note that $\Delta_0^c/W_\perp\sqrt{\zeta} = 0.9$. In summary, for $2/e < 2\Delta_0/W_\perp < 1$, the system is a semimetal: both the density of states at the Fermi energy and the order parameter Δ are nonzero.

Conducting polymers can hardly be described as highly oriented crystals: their morphology is very irregular and it can vary from sample to sample. Therefore, we expect that, whatever the intrinsic nature of the transition is, it will be affected by disorder. Moreover, because the doping process is discrete, it could be very difficult to distinguish a second-order transition from a first-order transition.

B. Antiferromagnetic ordering of the Peierls state

In the ferromagnetic case, the Peierls instability is readily suppressed by the interchain coupling, since it destroys the nesting of the Fermi surface. However, the system can often compensate the effect of the bending of the Fermi surface by properly choosing the three-dimensional ordering of the Peierls state. For instance, if the array of chains forms a square lattice, with nearest-neighbor coupling, antiferromagnetic ordering of the phase of the charge-density wave on neighboring chains produces perfect nesting at half-filling for arbitrary $W_\perp$. In contrast, any frustration in the system destroys this miraculous nesting. Such frustration arises if the polymer chains form a triangular lattice, if the effect of disorder is considered, or if further neighbor hopping is important. (In Na-doped polyacetylene, the polymer chains form a triangular lattice.)

To illustrate the effect of the interchain coupling, we consider the case where the chains form a triangular lattice which is tripartite and on which the Peierls state is frustrated. We further assume that the order parameter of the charge-density waves has a uniform amplitude Δ but phases 0, $2\pi/3$, and $4\pi/3$ on the three sublattices. For a given nearest-neighbor interchain hopping $t_\perp$, the interchain bandwidth is $W_\perp = 9t_\perp$ and the system is metallic, if $2\Delta_0 \leq W_\perp/2 + \mathcal{O}(W_\perp^2/W_\parallel)$. As a specific example, we consider a situation where the Peierls gap of the one-dimensional chain is such that $2\Delta_0/W_\parallel \ll 1$. Defining an effective interchain bandwidth as $\tilde{W}_\perp = W_\perp/2$, our main numerical result is that the system has a second-order transition to a metallic state as a function of Δ_0 or $\tilde{W}_\perp$. (i) For $2\Delta_0/\tilde{W}_\perp > 1$, the system is in the nonmetallic Peierls state whose order parameter is Δ_0. (ii) For $2/e \lesssim 2\Delta_0/\tilde{W}_\perp < 1$, it is a semimetal[24] with an incomplete Fermi surface and with a diminished order parameter Δ, less than Δ_0. Note that Δ vanishes rapidly with decreasing Δ_0 and, thus, with increasing doping density y. (iii) For $2\Delta_0/\tilde{W}_\perp \lesssim 2/e$, the system is an ordinary metal with no Peierls order ($\Delta = 0$).

Although the transition from the nonmetallic state to the metal is continuous, it is rapid and occurs over a narrow range of parameters. It may therefore easily appear as a first-order transition in real materials, since the doping process is discrete. It is intriguing to note that a pseudogap of magnitude 0.2 eV has been observed[5] in highly doped polyacetylene, for which $W_\parallel = 10$ eV and $W_\perp \lesssim 0.6$ eV.[25] If we take these numbers at face value, they imply that the system might be in the semimetallic phase.

C. Remarks

While an exact microscopic theory of the nonmetal–metal transition is a complicated problem because of local inhomogeneities and structural phase transitions, induced by counterions, we assume that the polymer chains form an ordered two-dimensional lattice which can be described by a mean-field-type Hamiltonian with effective interchain hopping matrix elements. Based on this approach, we argue that the metallic behavior observed in highly doped polyacetylene is a bona fide result of the interchain coupling.

We find that, if the three-dimensional Peierls order is frustrated, the system undergoes a transition to the metallic state once the Peierls gap of the corresponding one-dimensional system becomes small enough. A similar transition occurs on a square lattice near the half-filling when, for example, next-nearest-neighbor interchain hopping matrix elements are postulated—such terms might be important because the counterions modify the interchain couplings.[26] However, even if the nearest- and next-nearest-neighbor hopping matrix ele-

ments are equal, the square lattice is less frustrated than the triangular lattice in the sense that the transition to the metallic state occurs at higher doping density.

In this respect, a systematic study to determine whether the nonmetal–metal transition is sensitive to the arrangement of the counterions and thus to the lattice structure would be interesting and desirable. Unfortunately, such a comparison might be difficult to perform because doped polyacetylene has a complicated set of structural phase transitions as a function of doping and because the real samples are rather disordered.[27]

VI. CONCLUSIONS

In this study, we focused on various aspects of conducting polymers; in particular, we modeled them as quasi-one-dimensional crystals and used mean-field theory to compute their properties. Combining the experimental and the theoretical results, a coherent picture emerges of highly doped polymers as simple, albeit extremely anisotropic Fermi liquids.

At first sight, some experimental findings seem paradoxical within the Fermi-liquid picture, since the system exhibiting the basic metallic behavior still has features in common with the incommensurate Peierls state. We argue that the solution is to attribute different experimental probes to different features of real samples which, after all, have a very complex structure: The high conductivity, the spin susceptibility, and the linear specific heat, all of which are definite qualities of metals, arise from the three-dimensional nature of oriented metallic regions of polymer chains. Specifically, they are a manifestation of the presence of weakly interacting, charged quasiparticles with spin. On the other hand, we emphasize the well-known fact that the existence of the Peierls states is not requisite for having strong infrared activity: even in a metal, phonons can produce absorption peaks. Moreover, in dirty metals, which have poor conductivity, it is *common* to find a rich absorption spectrum.

We find three possible explanations for the presence of infrared-active modes in highly doped polymers:

(i) Counterions have a strong influence on the nature of the ground state: they can either enhance or completely destroy the Peierls state. Even if the average impurity density is homogeneous in a given sample, the metallic and Peierls states can coexist due to subtle microscopic differences in the arrangement of the counterions in different regions of the material. The infrared activity could then be due to nonmetallic regions of an otherwise metallic sample. It is also plausible that the more highly conducting samples are those with larger metallic fractions. These features could be tested experimentally by measuring the Pauli susceptibility and the Drude component of the optical absorption. If this explanation holds, the Drude component of the conductivity and the Pauli susceptibility should be increasing functions of the sample conductivity, while the oscillator strength associated with charged phonons (soliton-pinning modes) should be a decreasing function. Indeed, preliminary results[28] on Tsukamoto polyacetylene[29] reveal a Pauli susceptibility which is roughly three times larger than that of (considerably less conducting) Shirakawa polyacetylene at comparable doping densities.

(ii) For realistic three-dimensional band structures, the semimetallic phase intervenes between the nonmetallic (Peierls) and metallic (Fermi-liquid) phases. Because this seems to happen in the experimentally relevant range of parameters, the semimetallic state could explain both the metallic behavior and distinctive infrared-active modes.

(iii) We have shown that, in the metallic state, the Holstein process can easily produce infrared absorption of the observed intensity, although calculations in a more complex model including all the phonon modes would be necessary to determine whether it could produce the observed spectrum.

ACKNOWLEDGMENTS

It is our pleasure to thank A. Epstein and A. Heeger for fruitful discussions. This work was supported in part by the National Science Foundation Grant No. DMR-90-11803 and by the U.S. Department of Energy.

APPENDIX A

In the Born-Oppenheimer approximation, the total ground state, $|\Psi_0\rangle$, is assumed to have the factorized form

$$|\Psi_0\rangle = |\psi\rangle|\varphi_0\rangle \ , \tag{A1}$$

where $|\psi\rangle$ is the electronic ground state which depends parametrically on the lattice configuration $\{u_n\}$ and $|\varphi_0\rangle$ is the ground state of the lattice. The lattice dynamics is then given by the Hamiltonian[1]

$$\mathcal{H} = \frac{1}{2M}\sum_n p_n^2 + E(\{u_n\}) \ , \tag{A2}$$

where p_n is the momentum conjugate to u_n and E is the static energy, Eq. (2.3). Considering only small deviations from the equilibrium configuration $\{\bar{u}_n\}$, the energy $E(\{u_n\})$ can be expanded in a Taylor series about this point. In the harmonic approximation, we retain only the terms up to quadratic order. Defining the dynamic matrix as

$$D_{nm} = \left.\frac{\partial^2 E}{\partial u_n \partial u_m}\right|_{\{u_n\}=\{\bar{u}_n\}} \ , \tag{A3}$$

the Hamiltonian becomes

$$\mathcal{H} = \frac{1}{2M}\sum_n p_n^2 + \frac{1}{2}\sum_{nm} D_{nm} u_n u_m \ , \tag{A4}$$

apart from a constant term. There exists a complete set of normal-mode solutions, $|\varphi_k\rangle$, of Eq. (A4), that is,

$$\mathcal{H}|\varphi_k\rangle = \hbar\omega_k|\varphi_k\rangle \ . \tag{A5}$$

Each mode, $|\varphi_k\rangle$, describes a phonon with energy $\hbar\omega_k$.

In an absorption experiment, an external electromagnetic field couples to the current operator through the Hamiltonian

$$H' = -e\sum_n \rho_n \phi_n \ , \tag{A6}$$

where ϕ_n is the electric potential: $\mathcal{E}_n = -\nabla\phi_n$. Based on Fermi's golden rule, the absorption coefficient due to the one-phonon processes can be cast into the form of

$$\alpha_{\rm ad}(q,\omega)=\frac{\pi e^2}{2MVc}\sum_k \left|\sum_n h(n)\varphi_k(n)\right|^2\delta(\omega-\omega_k)\ , \tag{A7}$$

where

$$h(n)=\frac{1}{\mathcal{E}_0}\left[\sum_m \frac{\partial\langle\rho_m\rangle}{\partial u_n}\phi_m-\langle\rho_n\rangle\mathcal{E}_n\right]\ , \tag{A8}$$

V is the volume per polymer ring, $\mathcal{E}_0$ is the amplitude of the positive frequency part of the electric field with the wave vector q, and c is the velocity of light. The absorption is straightforwardly evaluated numerically once the equilibrium configuration is known.

The integrated infrared absorption can be written as

$$\mathcal{A}_{\rm ad}=\int d\omega\,\alpha_{\rm ad}(q,\omega)=\mathcal{A}_0\frac{m}{MN}\sum_n |h(n)|^2\ . \tag{A9}$$

The total oscillator strength for a one-dimensional conductor is[30]

$$\mathcal{A}_0=\frac{\pi}{2}\frac{N}{V}\frac{e^2}{mc}\ , \tag{A10}$$

and the band mass is given by $m=\pi\hbar^2/4t_0a^2$. For polyacetylene, $m\simeq 1.5m_e$, where m_e is the mass of the electron.

Finally, the external field $\mathcal{E}$ has to be specified. Since an infrared absorption experiment probes the system in the long-wavelength limit, we calculate the response as the wave vector of the field goes to zero. In a ring geometry, the field itself has to be periodic. For our purpose, it is then adequate to use the form $\mathcal{E}_n=\mathcal{E}_0 e^{iqna}$ with $q=2\pi/Na$, which is the smallest possible wave vector one can use.

APPENDIX B

We apply the standard model of an electron gas interacting with the phonons, i.e., the Hamiltonian in Eq. (2.1) with $V_n\equiv 0$ and $V_I=0$. Perturbation theory generates an expansion in series of powers of the coupling constant λ for the absorption coefficient. One can show that the leading order term behaves as

$$\alpha_H(\omega)=\frac{2\pi e^2}{\hbar^2 Vc}\frac{1}{\omega^3}\sum_{|k|\le k_F<|k+q|}|M_{kq}|^2(v_{k+q}-v_k)^2 \times\delta(\epsilon_{k+q}-\epsilon_k+\hbar\omega_q-\hbar\omega)\ . \tag{B1}$$

where the matrix element is given by the formula

$$M_{kq}=4\alpha\sqrt{\hbar/2NM\omega_q}\cos(ka+qa/2)\sin|q|a/2\ . \tag{B2}$$

We have defined the band energy $\epsilon_k=-2t_0\cos ka$, the band velocity $v_k=(1/\hbar)(\partial\epsilon_k/\partial k)$, and the phonon frequency $\omega_q=\omega_0\sin|q|a/2$. The expression for the absorption is the same as that of Allen's,[22] up to differences due to the dimensionality. The sums can be calculated once we notice that the most dominant contribution comes from the region around $|q|\sim 2k_F$. This implies that only those processes where optical phonons are exchanged and electrons scattered across the Fermi surface are important. Within this region, it is reasonable to assume that M_{kq} is approximately constant: $|M_{kq}|^2\sim 8\hbar\alpha^2/NM\omega_0$. Also, near the Brillouin-zone boundary the phonon-dispersion relation is almost flat which means that the relevant optical phonons have about the same frequency, namely ω_0. In particular, this approach is essentially the same as the Einstein model in which all phonons have the same frequency. These approximations, finally, lead to Eq. (4.2).

APPENDIX C

Below, we derive Eqs. (5.1) and (5.2).

Assuming ferromagnetic ordering of the Peierls state on adjacent chains, the one-electron energy levels can be written approximately as

$$\epsilon(\mathbf{k})=\epsilon_{\parallel}(k_{\parallel},\Delta)+\epsilon_{\perp}(\mathbf{k}_{\perp})\ , \tag{C1}$$

where $\parallel$ ($\perp$) refers to the direction parallel (perpendicular) to the chain axis. The crucial consequence is that the total density of states (per site), $\rho(\epsilon)$, factorizes into an in-chain, $\rho_{\parallel}$, and an interchain, $\rho_{\perp}$, part:

$$\rho(\epsilon)=\int_{-\infty}^{\infty}d\epsilon'\rho_{\parallel}(\epsilon')\rho_{\perp}(\epsilon-\epsilon')\ , \tag{C2}$$

where the factor of 2 arising from the spin degeneracy is included in $\rho_{\parallel}$. This is readily seen by Fourier transforming the total density of states.

Without loss of generality, we can define the energy scale so that

$$\int_{-\infty}^{\infty}d\epsilon\,\epsilon\rho_{\perp}(\epsilon)=0\ . \tag{C3}$$

Under these quite general conditions some precise predictions can be made. Specifically, consider the total energy per electron,

$$E_T(\Delta;W_{\perp})=\int_{-\infty}^{0}d\epsilon\,\epsilon\rho(\epsilon)+\text{the elastic energy}\ . \tag{C4}$$

Clearly E_T is independent of $W_{\perp}$ so long as $2\Delta>W_{\perp}$: $E_T(\Delta;W_{\perp})=E_T(\Delta;0)$. Moreover, it has a local minimum

$$E_T(\Delta_0;0)=E_T(0;0)-\frac{\Delta_0^2}{\pi W_{\parallel}}\ , \tag{C5}$$

where $2\Delta_0$ is the optimum value of the gap of the purely one-dimensional system.

The other minimum at $\Delta=0$ and fixed $W_{\perp}\neq 0$ can be seen as follows. Write

$$E_T(0;W_{\perp})=E_T(0;0)+\int_{-\infty}^{\infty}d\epsilon\,\rho_{\perp}(\epsilon)\int_{-\infty}^{-\epsilon}d\epsilon'(\epsilon+\epsilon')\rho_{\parallel}(\epsilon')\ , \tag{C6}$$

where we have used the property (C3). Since $\rho_\perp(\epsilon)$ is nonzero only in a narrow region around the point $\epsilon=0$, we can use the value $\rho_\parallel(0)=4/\pi W_\parallel$ for $\rho_\parallel(\epsilon)$ in this region. Therefore,

$$E_T(0;W_\perp)=E_T(0;0)-\zeta\frac{W_\perp^2}{\pi W_\parallel}\ , \tag{C7}$$

where ζ is defined in Eq. (5.3).

[1]See, for instance, A. J. Heeger, S. A. Kivelson, J. R. Schrieffer, and W. P. Su, Rev. Mod. Phys. **60**, 781 (1988); and references therein.

[2]W. P. Su, J. R. Schrieffer, and A. J. Heeger, Phys. Rev. Lett. **42**, 1698 (1987).

[3]H. Naarman, Synth. Met. **17**, 223 (1987); **22**, 1 (1987).

[4]H. H. S. Javadi *et al.*, Phys. Rev. B **43**, 2183 (1991); H. Kaneko *et al.*, J. Phys. Soc. Jpn. **62**, 3621 (1993).

[5]Y. H. Kim and A. J. Heeger, Phys. Rev. B **40**, 8393 (1989); D. B. Tanner *et al.*, Synth. Met. **28**, D141 (1989); X. Q. Yang *et al.*, Solid State Commun. **61**, 335 (1987).

[6]E. M. Mele and M. J. Rice, Phys. Rev. B **23**, 5397 (1981).

[7]E. M. Conwell and S. Jeyadev, Phys. Rev. Lett. **61**, 361 (1988).

[8]Z. G. Soos and S. Ramasesha, Phys. Rev. Lett. **51**, 2374 (1983); S. Mazumdar and S. N. Dixit, *ibid.* **51**, 292 (1983).

[9]S. A. Kivelson and M. I. Salkola, Synth. Met. **44**, 281 (1991).

[10]T. Holstein, Phys. Rev. **96**, 535 (1954).

[11]W-K. Wu and S. A Kivelson, Phys. Rev. B **34**, 5423 (1986).

[12]These parameters are $\alpha=4.1$ eV/Å, $K=21$ eV/Å^2, $t_0=2.5$ eV, $a=1.22$ Å, and $M=2.2\times10^{-26}$ kg. For instance, they give $\lambda=0.2$.

[13]S. A. Kivelson and D. E. Heim, Phys. Rev. B **26**, 4278 (1982).

[14]N. D. Mermin and H. Wagner, Phys. Rev. Lett. **17**, 1133; 1307(E) (1966).

[15]For polyacetylene, $\epsilon_\parallel=11.5\epsilon_0$ and $\epsilon_\perp=2.5\epsilon_0$. This implies that $\gamma=2.1$.

[16]M. Winokur *et al.*, Phys. Rev. Lett. **58**, 2329 (1987).

[17]S. A. Kivelson and A. J. Heeger, Synth. Met. **22**, 371 (1988).

[18]A. J. Heeger and J. R. Schrieffer, Solid State Commun. **48**, 207 (1983).

[19]For $l=4a$, we get two scaling trajectories since there exist two different kinds of rings: ones which have counterions equally spaced ($N=60$ and 120), others which have always two counterions whose separation is $6a$ ($N=30$ and 90). However, the difference vanishes as $N\rightarrow\infty$ and both trajectories extrapolate about to the same point.

[20]E. J. Mele and J. C. Hicks, Phys. Rev. B **32**, 2703 (1985).

[21]For $U=0$, $m^*=5.2m_e$, which is close to estimates obtained by other methods (Ref. 1).

[22]P. B. Allen, Phys. Rev. B **3**, 305 (1971).

[23]Z. H. Wang, C. Li, E. M. Scherr, A. G. MacDiarmid, and A. J. Epstein, Phys. Rev. Lett. **66**, 1745 (1991).

[24]A semimetallic phase is not a new idea; see, for example, K. Yamaji, J. Phys. Soc. Jpn. **51**, 2787 (1982).

[25]D. Moses *et al.*, Phys. Rev. B **26**, 3361 (1982). Note that, to our knowledge, there exist no reliable experimental estimates for the interchain hopping matrix elements in doped polyacetylene, although theoretical estimates suggest that they are modified considerably by doping; see Ref. 26.

[26]R. J. Cohen and A. J. Glick, Phys. Rev. B **42**, 7659 (1990).

[27]See, for example, P. A. Heiney *et al.*, Phys. Rev. B **44**, 2507 (1991); M. J. Winokur *et al.*, *ibid.* **45**, 9656 (1992).

[28]A. J. Epstein (private communication).

[29]J. Tsukamoto, Adv. Phys. **41**, 509 (1992).

[30]S. A. Kivelson, T-K. Lee, Y. R. Lin-Liu, I. Peschel, and L. Yu, Phys. Rev. B **25**, 4173 (1982).

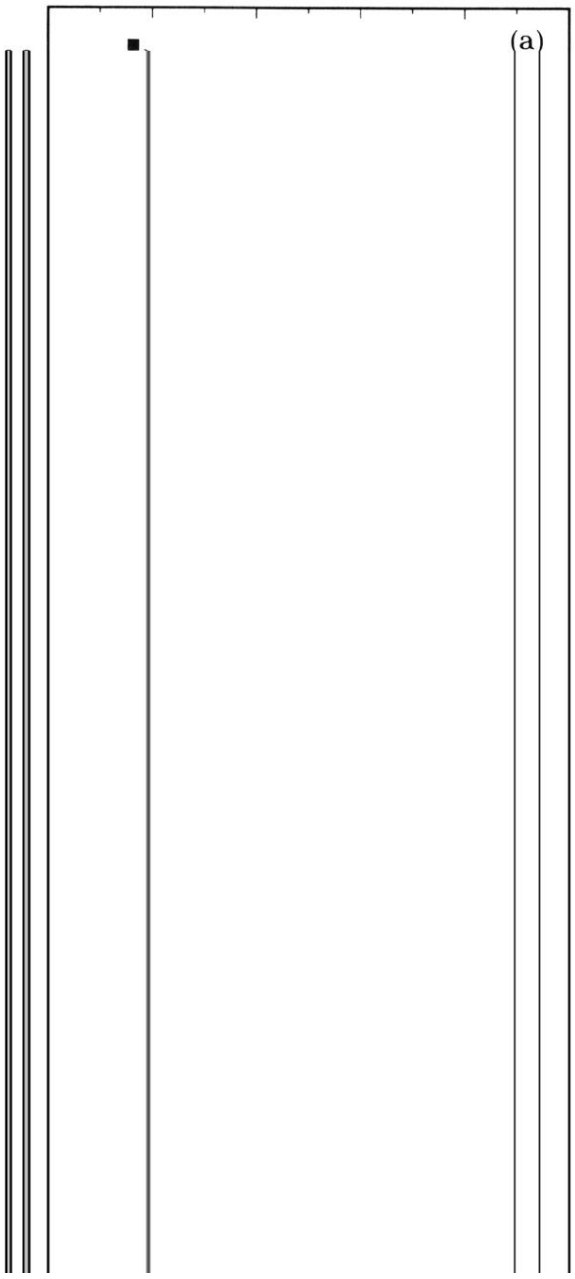
(a)

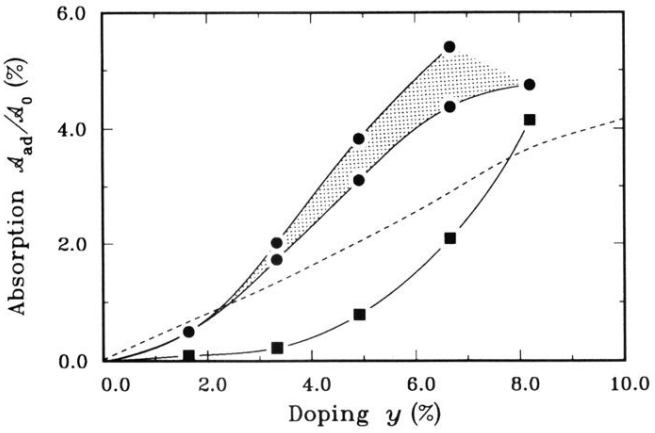

FIG. 4. The integrated absorption $\mathcal{A}_{ad}$ for adiabatic processes as a function of doping density, y, for $U=t_0$, and $v_I=t_0$. The symbols are as follows: the dashed line denotes the counterion-free case, l/a=odd (■) and l/a=even (●). Computations are based on those values of the separation between counterions, l, which are summarized in Table I and approximately satisfy the relation $l=a/(3y)$. The shadowed regions emphasize the effect of a change of $2a$ in l. $\mathcal{A}_0$ is the total oscillator strength, Eq. (A10).